Journal of Energetic Materials
Publication details, including instructions for authors and subscription information:
http://www.informaworld.com/smpp/title~content=t713770432

Pyrolysis GC-FTIR studies of a LOVA propellant formulation series

R. A. Pesce-rodriguez[a]; F. J. Shaw[a]; R. A. Fifer[a]
[a] US Army Ballistic Research Laboratory, Aberdeen Proving Ground, MD

To cite this Article Pesce-rodriguez, R. A. , Shaw, F. J. and Fifer, R. A.(1992) 'Pyrolysis GC-FTIR studies of a LOVA propellant formulation series', Journal of Energetic Materials, 10: 4, 221 — 250
To link to this Article: DOI: 10.1080/07370659208018924
URL: http://dx.doi.org/10.1080/07370659208018924

PYROLYSIS GC-FTIR STUDIES OF A LOVA PROPELLANT FORMULATION SERIES

R.A. Pesce-Rodriguez, F.J. Shaw, and R.A. Fifer

US Army Ballistic Research Laboratory
Aberdeen Proving Ground, MD 21005-5066

ABSTRACT

Pyrolysis - gas chromatography - Fourier transform infrared (P-GC-FTIR) spectroscopy has been used to examine the pyrolysis product distributions of a LOVA propellant formulation series. The propellants in the series were composed of oxidizer (HMX or RDX), polymeric binder (GAP, HTPB, BAMO/AMMO, or BAMO/THF), and plasticizer (BTTN or TMETN). Trends in product distribution as a function of formulation, as well as a correlation between pyrolysis products and performance data, were identified. In general, pyrolysis product distributions were found to be most strongly affected by the presence and type of plasticizer.

Journal of Energetic Materials Vol. 10, 221-250 (1992)
Published in 1992 by Dowden, Brodman & Devine, Inc.

INTRODUCTION

A considerable amount of information has been published concerning the mechanisms and products of the thermal decomposition of the nitramines cyclotrimethylene trinitramine (RDX) and cyclotetramethylene tetranitramine (HMX). References 1-3 are useful reviews of the literature. Until recently, these studies primarily involved measurement only of the permanent gases (CO_2, NO_2, NO, CH_2O, HCN, N_2O, N_2, etc.) in the products, or involved mass spectral studies under vacuum conditions where it is difficult to distinguish pyrolysis from ionization-induced fragmentation of vaporized nitramine molecules. During the last several years, two developments have led to the identification of larger fragments in the pyrolysis products. One is the application of fused silica capillary column GC techniques.[4-9] The other involves new mass spectral techniques involving time-of-flight measurements to determine the parent peak leading to each ion fragment,[10,11] or employing atmospheric pressure chemical ionization and tandem mass spectrometric techniques to minimize vaporization and provide information on the structures of observed product masses.[12]

The majority of the published studies have concentrated on the development of mechanisms to explain the formation of the observed decomposition products. There have been very few attempts to correlate pyrolysis product distributions with large scale performance tests such as ignitability, impact sensitivity, or burn rate. Since definitive mechanistic information has not been forthcoming for the nitramines and nitramine propellants, the search for correlations may be a more fruitful approach. Mechanisms are not required, only a correlation of one or more features in the pyrolysis product distributions with the performance property of interest. Once such a correlation is found, the pyrolysis measurement becomes a small scale screening test for the desired performance property, one that perhaps does not require fabrication on a large scale, or that might require only unprocessed mixtures of potential ingredients. Also, the correlation may suggest rules that can be used in expert systems for computer assisted formulations design and properties prediction.[13] Correlating pyrolysis product distributions with performance is analogous to reported correlations between LOVA (LOw Vulnerability Ammunitions) propellant sensitivity with binder/acid DSC decomposition tempera-

ture.[14,15] The information content in a product distribution measurement, where perhaps 15 or 20 products are measured, is much greater than in a thermokinetic measurement where only a single property (e.g. decomposition temperure) is measured, so there should be an even greater likelihood of finding a useable correlation.

The principle reason why pyrolysis-performance correlations have not been previously attempted is that a suitable series of systematically varied propellant formulations, with properly documented performance measurements, has not been available. Such a LOVA formulation series was recently developed at the Naval Weapons Center (NWC), China Lake, by Dr. Rena Yee,[16-18] who provided both samples and performance test data for this study. In the formulation series, oxidizer and binder were systematically varied. Performance test results include burn rate, impact sensitivity and time-to-ignition for radiative heating. This formulation series contains either RDX or HMX as the oxidizer and one of the following polymers: hydroxy-terminated polybutadiene (HTPB), glycidyl azide polymer (GAP), 3,3-bis-azido-methyl oxetane/tetrahydrofuran (BAMO/THF) copolymer, or 3,3-bis-azidomethyl oxetane/3,3-bis-

azidomethyl-3-methyl oxetane (BAMO/AMMO) copolymer. The azido polymers were plasticized with either trimethylolethane trinitrate (TMETN) or 1,2,4-butane trinitrate (BTTN). The composition of each formulation is given in Table 1. Pure HMX, RDX, GAP, HTPB and plasticizers were also analyzed.

TABLE 1

Composition of Propellant Formulations

Sample	RDX	HMX	Polymer	Type	Plasticizer	Type
	(Composition in weight-%)					
4	74.8	0.0	6.3	GAP	18.9	TMETN
8	68.4	0.0	31.6	GAP	0.0	
9	65.9	0.0	11.5	GAP	22.6	BTTN
14	0.0	69.7	30.3	GAP	0.0	
15	0.0	0.0	50.0	GAP	50.0	BTTN
16	75.0	0.0	25.0	HTPB	0.0	
17	0.0	76.0	24.0	HTPB	0.0	
18	0.0	0.0	50.0	GAP	50.0	TMETN
19	65.0	0.0	17.5	GAP	17.5	BTTN
20	0.0	66.3	16.8	GAP	16.9	BTTN
21	0.0	67.6	16.2	BAMO/THF	16.2	BTTN
22	0.0	68.2	15.9	BAMO/AMMO	15.9	TMETN
23	0.0	68.6	15.7	BAMO/THF	15.7	TMETN
24	0.0	68.3	15.8	GAP	15.9	TMETN
25	67.1	0.0	16.6	GAP	16.4	TMETN

Although the initial purpose of this investigation was to identify correlations between pyrolysis product distributions and ignition times, several other trends related to propellant formulation were observed and will also be discussed here. (For more detailed exper-

imental results see refence 19.) The sample set provided the opportunity to observe not only the correlations of pyrolysis product distribution with ignition time, but also the effect of formulation on pyrolysis product distribution. It is hoped that the results of this investigation will be useful to those interested in propellent design and performance prediction.

EXPERIMENTAL

All samples were pyrolyzed using a Chemical Data Systems (CDS) Model 122 Pyroprobe® connected via a heated interface chamber to the splitless injector of a Hewlett Packard 5965 GC-FTIR equipped with a capillary column and liquid nitrogen cooled Mercury Cadmium Telluride (MCT) detector (Hewlett Packard Model 5965A infrared detector).

The pyrolysis sample (ca. 1 mg) was placed in a quartz tube packed with glass wool. The tube was then inserted into a coil-type Pyroprobe®. The probe was inserted into the heated interface which was continuously being swept with carrier gas. Once enough time had elapsed to allow the carrier gas to sweep all air from the interface compartment and to allow the sample to reach thermal equilibrium, the sample was flash heated to the pyrolysis temperature and held at that

temperature for 20 seconds. The pyrolysis products then passed through the splitless injector into the capillary column, which separated the products for detection and identification. As each component eluted from the capillary column, it passed through a light pipe in the beam of an interferometer for spectroscopic analysis by Fourier transform infrared (FTIR) spectroscopy.

Other chromatographic and spectroscopic conditions are given as follows: GC conditions: Quadrex capillary column, 0.32 mm x 25 m x 3 μm OV-17 film; oven program: 50°C for 3 min, then 50→200°C at 10 deg/min; injector and interface chamber held at 100°C. FTIR conditions: transfer lines and light pipe held at 200°C; three interferograms per second were continuously collected at 8 cm^{-1} resolution during the chromatographic run. Real-time chromatograms (IR response vs time) were recorded via application of the Gram-Schmidt algorithm[20]; the FTIR spectrum for each peak was available for analysis or for automated search of the EPA library of approximately 5,000 vapor phase spectra.

Each of the samples was pyrolyzed at both a low and high temperature. For the low temperature experiments, RDX formulations and formulations of GAP/plasti-

cizer (no oxidizer) were pyrolyzed at 400°C, while HMX formulations were pyrolyzed at 500°C. For the high temperature experiments, all samples were pyrolyzed at 1000°C. Low temperature experiments were not carried out for GAP and HTPB because of their thermal stability. Thermocouple measurements indicated that the actual temperatures experienced by samples in the quartz tubes were 150-200°C lower than the Pyroprobe® set temperatures. The low temperature experiments were, therefore, just above the melting points of RDX and HMX (204 and 280°C, respectively). Three experiments were carried out for each of the samples at each of the two temperatures to insure reproducibility.

Gas chromatograms were generated by application of the Gram-Schmidt algorithm to the FTIR detector output. Peaks were then identified by examination of the associated FTIR spectra. A small fraction of the peaks was directly identified by an automated search of the EPA library of vapor phase spectra. Software for this search was provided by the manufacturer.

Retention times were corrected to give the permanent gas peak at 0.0 min. Quantification of pyrolysis products was based on GC peak areas and is reported in area percent in Tables 2, 3, 4, and 5. Exceptions to

this are the individual permanent gas products which are not readily quantified by GC peak area because they elute within a few seconds of each other and appear as a single GC peak. For this reason, individual permanent gas quantities were calculated from FTIR absorbance and are given in normalized absorbance units (Tables 6 and 7). To calculate these normalized absorbance values, all FTIR spectra under the permanent gas GC peak were first summed to yield a single spectrum. The absorbance of the largest band for each permanent gas in this spectrum was then divided by the sum of the absorbances of the largest band for each gas. The bands chosen for each gas are given as follows: CH_4, 3016 cm^{-1}; CH_2O, 2804 cm^{-1}; CO_2, 2363 cm^{-1}; N_2O, 2238 cm^{-1}; CO, 2111 cm^{-1}; NO, 1912 cm^{-1}.

It must be stressed that all reported values are uncalibrated, relative quantities that are only used to identify variations in pyrolysis product distributions. Magnitudes of absorbance, as well as GC peak areas, for different compounds are not comparable due to differences in infrared absorption coefficients.

Although the data reported here represent one of the most comprehensive investigations of pyrolysis product distribution for propellant formulations to

date, several products are notably absent. Most of these products reacted before reaching the light pipe, and therefore could not be detected. These include highly reactive species such as NO_2, radicals, and ions. Other species, such as N_2 and H_2, do not absorb in the infrared region,and therefore were not detected. In spite of this drawback, pyrolysis GC-FTIR is a powerful technique which complements the more commonly used GC-MS methods, with which no analysis of the permanent gases would be possible with normal unit mass resolution. The reason for this is that there are a number of unfortunate coincidences in the ion fragment patterns for many of the commonly observed permanent gases. For example, m/z 28 could be CO or N_2, m/z 30 could be CH_2O or NO, m/z 44 could be N_2O or CO_2, etc. With GC-FTIR this is not a problem; most of the gases have more than one absorption band, and for each gas there is at least one IR band for which there is no interference from other species.

RESULTS

Pyrolysis Product Distributions: The primary experimental data obtained from these experiments are GC peak areas. Retention times and FTIR spectra aid in the identification of pyrolysis products. Based on

such information, product distributions for 15 different propellant formulations and 4 of the pure components (RDX, HMX, GAP and HTPB) have been determined. Pyrolysis products have been divided into several catagories, i.e. permanent gases (CO_2, N_2O, CO, NO, CH_2O, CH_4), HCN, water, nitrates (RNO_3), nitro compounds (RNO_2), isocyanates (HNCO, RNCO), carboxylic acids (RCOOH), ketones, esters, amides, and aldehydes. Permanent gases and other molecules such as acetone, acrolein, acetaldehyde, acetic acid, formic acid, and triazine were identified from their FTIR spectra. Other less readily identifiable products are classified in this report by their functionalities. Tables 2 and 3 summarize the P-GC-FTIR results for low and high temperature experiments, respectively.

By far, the most abundant pyrolysis products for all formulations are the permanent gases. The remainder of the products are generated by most or some of the formulations. Triazine results from incomplete pyrolysis of oxidizer. Nitrates are derived from the energetic plasticizers. Isocyanates, other than HNCO, are likely generated from the curing agents (isopherone diisocyanate and N-100) which are used to cross-link HTPB and GAP.

TABLE 2

Low Temperature Pyrolysis Products as Eluted on GC

Retention Time (min)	4	Area %	8	Area %	9	Area %	14	Area %	15	Area %	16	Area %	17	Area %	18	Area %
0.0	PG	79.9	PG	46.7	PG	81.0	PG	56.2	PG	84.4	PG	58.6	PG	69.6	PG	67.1
0.5	H2O		HNCO	4.0	H2O	1.0	HCN				H2O		HCN			
1.0			acrolein	1.5	HNCO	1.0	H2O						H2O		acetaldehyde	10.0
1.5			triazine	21.2	acrolein	1.5									HNCO	2.2
2.0			acetic				acrolein	1.0	acetone	2.7	triazine	14.6	acrolein	1.0	acetone	4.7
2.5			acid	2.2	oxadiazole	0.4	oxadiazole	1.0	?	0.6						
3.0	acetic	2.6	formic								formic				acrolein	2.4
3.5	acid		acid	4.8	formic	0.4			isocyanate	0.4	acid	0.5				
4.0			ketone*	19.0	acid				acetic		ester	3.0			nitro-	0.9
4.5			ketone	2.2	nitro-	0.4			acid	4.0					methane	
5.0					methane		nitro-	1.0	formic	1.0					acetic	5.7
5.5							methane		acid						acid	
6.0	ester	1.2			ketone	1.0	aldehyde	2.5			ester#	16.7	triazine	5.7		
6.5							triazine	1.4			ketone*	6.4				
7.0																
7.5	nitrate	1.0									nitro-	5.6				
8.0									ester	0.5	formamine				ester	1.5
8.5									isocyanate	0.6	ketone	2.3				
9.0					ketone	2.0			ester	1.4					nitro-	1.0
9.5															alkane	
10.0									ketone	2.6						
10.5	ketone	1.1							isocyanate	0.5						
11.0					isocyanate	0.4	ketone*	7.8					ketone*	7.5		
11.5	isocyanate	1.1			ester#	10.2					N-methyl-	0.4	N-methyl-	11.3		
12.0	nitrate	10.3					N-methyl-	14.5			formamide		formamide			
12.5	ketone	1.6					formamide		ketone	0.2					isocyanate	1.4
13.0																
13.5					nitro-	0.8										
14.0					formamine											
14.5							ether	6.7								
15.0															isocyanate	1.6
15.5																
16.0															isocyanate	1.6
16.5							nitro-	6.9					nitro-	5.1		
17.0							formamine		ketone	0.2			formamine			

19	Area %	20	Area %	21	Area %	22	Area %	23	Area %	24	Area %	25	Area %	RDX	Area %	HMX	Area %	Retention Time (min)
PG	90.4	PG	80.7	PG	85.0	PG	70.0	PG	57.2	PG	71.3	PG	82.6	PG	29.9	PG	92.1	0.5
		HCN		HCN		HCN		HCN		HCN				formic acid	4.6	HCN		1.0
		H2O		H2O		H2O		H2O		H2O				oxadiazole	4.2	H2O		1.5
		acrolein	1.4			acetone	1.1							triazine	8.1			2.0
ester	1.3													ketone*	7.8			2.5
														N-methyl-				3.0
						acrolein	1.4			nitro-	0.4			formamide	1.4			3.5
						nitro-	0.4			methane				ketone	0.8			4.0
						methane				acetic	0.8	nitrate	1.6	ester#	26.9			4.5
nitrate	2.6									acid				ester	5.2			5.0
isocyanate	2.9											nitrate	8.1					5.5
nitrate	1.9													ester	4.6			6.0
		triazine	1.4	triazine	0.3	triazine	6.9			triazine	2.5	isocyanate	5.7	CN hetero-	2.5			6.5
										acetic	3.4			cycle		triazine	2.3	7.0
								triazine	3.2	acid				ketone	4.1			7.5
								formic	1.5			ketone	1.8					8.0
		formic	0.8	formic	2.4			acid		formic	3.1							8.5
		acid		acid						acid								9.0
																		9.5
		ketone	6.4															10.0
				ketone	4.3					ketone	16.8							10.5
		ketone	7.4	ketone	7.9			ketone*	7.0									11.0
						ketone	19.5											11.5
								ketone	29.5							ketone	2.3	12.0
																		12.5
																		13.0
																		13.5
																		14.0
																		14.5
																ketone	3.4	15.0
								ketone	1.6									15.5
																		16.0
																		16.5
																		17.0

Key: PG permanent gases
*,# indicates compound has infrared spectrum identical to that of other compounds with same notation
] overlapping peaks; GC peak areas have been summed

NOTE: Pyroprobe set temperature: 400°C for RDX formulations, 500°C for HMX formulations. Retention times rounded off to nearest 0.5 min. Numbers appearing to the right of products are GC peak areas in area-percent.

TABLE 3
High Temperature Pyrolysis Products as Eluted on GC

Retention Time (min)	4	Area %	8	Area %	9	Area %	14	Area %	15	Area %	16	Area %	17	Area %	18	Area %	19	Area %	20	Area %
0.0	PG		PG		PG		PG		PG	59.6	PG		PG	61.4	PG	43.7	PG		PG	
0.5	HCN	68.9			HCN	85.9									HCN		HCN	64.2	HCN	59.4
1.0	H2O		H2O	69.8	H2O		H2O	74.2	acetaldehyde	22.4	H2O	91.6			acetaldehyde	15.3	H2O		H2O	
1.5							HNCO	0.2												
2.0	HNCO	0.6			HNCO	1.4			HNCO	3.8	acrolein	0.8			HNCO	3.7	HNCO	1.6		
2.5									ketone	4.5			acrolein	0.6	acetone	7.5	acrolein	0.7		
3.0							?	4.4					triazine	2.0						
3.5											oxadiazole	0.2	formic	0.2	acrolein	3.7			triazine	2.1
4.0			triazine	6.3									acid						acetic	1.1
4.5																			acid	
5.0					triazine	3.6					benzene	0.3			nitro-	2.2				
5.5											aldehyde	0.5			methane					
6.0					formic	0.1	triazine	2.2	isocyanate	0.6	triazine	5.7			acetic acid	9.3			formic	11.6
6.5					acid				acetic	4.5									acid	
7.0	triazine	6.9							acid											
7.5							formic	1.5			toluene	0.2	ketone*	26.4	ester	1.9				
8.0							acid										triazine	9.0		
8.5			ketone	17.1											nitro-	1.5			ketone*	17.6
9.0									carboxylic	0.6					alkane				acetamide	1.5
9.5					ketone	7.9			acid										amide	0.5
10.0													nitro-						amide	0.4
10.5			nitro-	3.6							ketone	0.3	formamine	0.6	ester	1.1			nitro-	0.2
11.0			formamine										CN hetero-	0.5					formamine	
11.5													cycle		isocyanate	1.1			CN hetero-	0.4
12.0							ketone	14.5	isocyanate	1.3									cycle	
12.5			isocyanate	0.6									ketone	2.9	triacetin	1.9			nitro-	0.2
13.0					ketone	1.1					ketone	0.3	a	0.5					alkane	
13.5											ketone	0.3			ketone	1.5			amide	2.1
14.0															ketone	1.5	ketone	1.8		
14.5	ketone	1.6											ketone	4.2						
15.0									isocyanate	1.3					isocyanate	3.4			amide	2.6
15.5				2.6																
16.0									isocyanate	1.3										
16.5															ketone	0.7	ketone	2.7		
17.0																			amide	0.5

21	Area %	22	Area %	23	Area %	24	Area %	25	Area %	RDX	Area %	HMX	Area %	GAP	Area %	HTPB	Area %	Retention Time (min)
PG		PG		PG	62.8	PG		PG		PG	26.4	PG		PG	38.7	PG	18.6	0.0
HCN	72.8		71.0			HCN	74.6	HCN	72.4	HNCO	24.2	HCN	44.3			monomer	22.7	0.5
		H2O				H2O		H2O		oxadiazole	3.1	H2O		acetaldehyde	28.1			1.0
										triazine	4.3	HNCO	3.2	HNCO	7.0			1.5
								HNCO	0.5			acetone	1.3	acetone	4.8			2.0
																		2.5
		triazine	2.5	triazine	3.3	triazine	1.5			ketone*	4.1							3.0
triazine	4.0	acetic	3.2	acetic	2.5	acetic	1.5			ketone	0.6	oxadiazole	1.3					3.5
acetic	1.0	acid		acid		acid				acrolein	0.3					dimer	14.4	4.0
acid										ester#	21.9							4.5
formic	5.0	formic	3.8			formic	2.5			ester	5.3							5.0
acid		acid				acid										alkane	2.3	5.5
				formic	7.1													6.0
				acid				acetic				formic	2.9					6.5
								acid	0.2	ketone	7.8	acid						7.0
ketone*	13.3							triazine	7.4							aromatic	3.0	7.5
		ketone*	13.3	ketone*	14.6	ketone*	14.8											8.0
acetamide	1.0	acetamide	1.3	acetamide	2.0	acetamide	1.5									alkene	3.3	8.5
		amide	0.2	amide	0.4													9.0
amide	0.3			lactone	0.4	ketone	0.9									alkene	2.3	9.5
				ketone	0.9													10.0
ketone	0.1					amide	1.0							imine	3.2			10.5
nitro-		ketone	1.9	nitro-								ketone*	6.7	n-methyl-				11.0
formamine	0.6			formamine	0.7									formamide	4.4			11.5
CN hetero-	0.2			ester	0.2							acetamide	12.8	acetamide	6.3			12.0
cycle		ketone	1.1	CN hetero-				ketone*	6.7									12.5
				cycle	0.3													13.0
ketone	1.0			ketone	2.5			acetamide	12.7									13.5
				a	0.1													14.0
ketone	0.6					a	0.1					ester#	24.5					14.5
		a	1.0											ketone	3.8	alkene	11.3	15.0
				N-methyl-	2.0	amide	0.9									alkene	4.5	15.5
				formamide								nitro				alkene	6.0	16.0
												formamine	2.7			alkene	3.8	16.5
amide	0.1											ketone	0.7	isocyanate	3.6	isocyanate	13.6	17.0

Key: PG permanent gases
*,# indicates compound has infrared spectrum identical to that of other compounds with same notation
] overlapping peaks; GC peak areas have been summed

NOTE: Pyroprobe set temperature: 1000°C for all formulations. Retention times rounded off to nearest 0.5 min. Numbers appearing to the right of products are GC peak areas in area-percent.

Pyrolysis experiments were run at both "low" (400°C or 500°C, for RDX and HMX formulations, respectively) and "high" (1000°C, for all formulations) temperatures. Tables 4 and 5 summarize GC area-percent values for all low and high temperature pyrolysis products except individual permanent gas products, which are given in normalized absorbance units in Tables 6 and 7, respectively.

Selection of Performance Data for Correlation with Pyrolysis Products: Performance test results[17] are given in Table 8, and include impact sensitivity and burn rate measurements as well as "first light" and "go/no-go" ignition times. First light measurements indicate initial emission whereas go/no-go measurements indicate the time of laser stimulus necessary for 50% of the samples to sustain combustion after removal of the stimulus. Theoretical specific impulse was also provided. Examination of burn rate and impact sensitivity vs specific impulse indicates a strong correlation and suggest that these two measurements are thermodynamically controlled. First light and go-no go ignition times do not show such a correlation and are therefore not believed to be thermodynamically controlled, making them suitable choices for possible

TABLE 4

Pyrolysis Products for Low Temperature Experiments

Sample No.	PG, HCN and H20	Triazine	Nitro-Alkane	Nitrate	Isocyanate	Carboxylic Acid	Ketone	Ester	Amide	Aldehyde	Other
	(GC area-percent)										
4	79.9	0.0	0.0	11.3	2.7	2.6	2.7	1.2	0.0	0.0	
8	46.7	21.2	0.0	0.0	4.0	7.0	21.2	0.0	0.0	0.0	
9	81.0	0.0	1.2	0.4	1.4	0.4	3.0	10.2	0.0	1.5	0.4(a)
14	56.2	1.4	7.9	0.0	0.0	0.0	7.8	0.0	14.5	3.5	1.0(a), 6.7(b)
15	84.4	0.0	0.0	0.0	1.5	5.0	6.7	1.9	0.0	0.0	0.6(d)
16	50.6	14.6	5.6	0.0	0.0	0.5	8.7	19.7	0.4	0.0	
17	69.6	5.7	5.1	0.0	0.0	0.0	7.5	0.0	11.5	1.0	
18	67.1	0.0	1.9	0.0	5.2	5.7	4.7	3.1	0.0	12.4	
19	90.6	0.0	0.0	4.5	2.9	0.0	0.0	1.3	0.0	0.0	
20	80.7	1.4	0.0	0.0	0.0	0.8	15.8	0.0	0.0	1.4	
21	85.0	0.3	0.0	0.0	0.0	2.4	12.3	0.0	0.0	0.0	
22	70.0	6.9	0.4	0.0	0.0	0.0	20.6	0.0	0.0	1.4	
23	57.2	3.2	0.0	0.0	0.0	1.5	38.1	0.0	0.0	0.0	
24	71.3	2.5	0.4	0.0	0.0	7.3	18.8	0.0	0.0	0.0	
25	82.8	0.0	0.0	9.7	5.7	0.0	1.8	0.0	0.0	0.0	
RDX	29.9	8.1	0.0	0.0	0.0	4.6	12.7	36.7	1.4	0.0	4.2(a), 2.5(c)
HMX	92.1	2.3	0.0	0.0	0.0	0.0	5.7	0.0	0.0	0.0	

a) oxidiazole, b) ether, c) carbon-nitrogen heterocycle, d) unknown

TABLE 5

Pyrolysis Products for High Temperature Experiments

Sample No.	PG, HCN and H20	Triazine	Nitro-Alkane	Nitrate	Isocyanate	Carboxylic Acid	Ketone	Ester	Amide	Aldehyde	Other
	(GC area-percent)										
4	88.9	8.9	0.0	0.0	0.6	0.0	1.6	0.0	0.0	0.0	
8	69.8	6.3	3.6	0.0	0.6	0.0	19.7	0.0	0.0	0.0	
9	85.9	3.6	0.0	0.0	1.4	0.1	9.0	0.0	0.0	0.0	
14	74.2	2.2	0.0	0.0	0.2	1.5	16.5	0.0	0.0	0.0	4.4(d)
15	59.6	0.0	0.0	0.0	8.3	5.1	4.5	0.0	0.0	4.5	
16	91.6	5.7	0.0	0.0	0.0	0.0	0.9	0.0	0.0	1.1	0.2(a), 0.5(b)
17	61.4	2.0	0.6	0.0	0.0	0.2	33.5	0.0	0.0	0.6	0.5(c), 0.5(e)
18	43.7	0.0	3.7	0.0	8.2	9.3	11.2	4.9	0.0	19.0	
19	84.2	9.0	0.0	0.0	1.6	0.0	4.5	0.0	0.0	0.7	
20	59.4	2.1	0.4	0.0	0.0	12.7	17.6	0.0	7.6	0.0	0.4(e)
21	72.8	4.0	0.6	0.0	0.0	6.0	15.0	0.0	1.4	0.0	0.2(e)
22	71.0	2.5	0.0	0.0	0.0	7.0	16.3	0.0	1.5	0.0	1.0(c)
23	62.8	3.3	0.7	0.0	0.0	9.6	18.0	0.4	4.6	0.0	0.1(c), 0.3(e)
24	74.8	1.5	0.0	0.0	0.0	4.0	15.7	0.0	3.4	0.0	0.1(c)
25	72.4	7.4	0.0	0.0	0.5	0.2	6.7	0.0	12.7	0.0	
RDX	26.4	6.3	0.0	0.0	24.2	0.0	12.5	27.2	0.0	0.3	3.1(a)
HMX	44.3	0.0	2.7	0.0	3.2	2.9	8.2	24.5	12.8	0.0	1.3(a)
GAP	38.7	0.0	0.0	0.0	10.6	0.0	8.6	0.0	10.7	28.1	3.2(f)
HTPB	10.6	0.0	0.0	0.0	13.6	0.0	0.0	0.0	0.0	0.0	(g)

a) oxidiazole, b) aromatic, c) methylimine diacetonitrile, d) unknown, e) carbon-nitrogen heterocycle, f) imine

g) also gave 22.7% butadiene monomer, 14.4% butadiene dimer, 2.3% unidentified alkane, 33.2% unidentified alkene, and 3.0% unidentified aromatic.

TABLE 6

Individual Permanent Gas Pyrolysis Products for Low Temperature Experiments

Sample No.	CH4	CH2O	CO2	N2O	CO	NO
	(Normalized IR Absorbance)					
4	0.00	0.14	0.45	0.25	0.01	0.03
9	0.03	0.00	0.43	0.38	0.06	0.09
14	0.06	0.00	0.37	0.43	0.06	0.08
17	0.03	0.00	0.38	0.45	0.04	0.09
19	0.00	0.07	0.45	0.34	0.03	0.05
20	0.05	0.00	0.39	0.41	0.07	0.09
21	0.04	0.00	0.40	0.40	0.07	0.09
22	0.07	0.00	0.38	0.41	0.06	0.09
24	0.06	0.00	0.39	0.42	0.06	0.08
25	0.00	0.16	0.32	0.32	0.02	0.05

TABLE 7

Individual Permanent Gas Pyrolysis Products for High Temperature Experiments

Sample No.	CH4	CH2O	CO2	N2O	CO	NO
	(Normalized IR Absorbance)					
4	0.05	0.00	0.39	0.40	0.07	0.12
9	0.03	0.00	0.43	0.40	0.06	0.08
14	0.08	0.00	0.38	0.47	0.07	0.09
17	0.13	0.00	0.40	0.34	0.05	0.09
19	0.07	0.00	0.40	0.37	0.07	0.10
20	0.06	0.00	0.45	0.33	0.07	0.09
21	0.06	0.00	0.41	0.35	0.07	0.10
22	0.08	0.00	0.39	0.37	0.07	0.10
24	0.08	0.00	0.40	0.33	0.08	0.11
25	0.06	0.00	0.41	0.37	0.07	0.09

TABLE 8
Propellant Performance Test Results[17]

Sample	Isp (a)	Impact	Burn Rate (b)	Ignition Times							
				Go/No-Go (ms)				First Light (ms)			
	(1/s)	(cm)	(mm/s)	60(c)	100(c)	150(c)	200(c)	60(c)	100(c)	150(c)	200(c)
4	257.8	13.6	7.9	11.5	5.8	4.7	8.0	10.3	5.1	2.4	1.5
8	235.4	30.2	6.6	NA	NA	NA	NA	NA	NA	NA	NA
9	257.0	15.6	7.6	9.9	5.1	3.4	6.1	8.9	4.2	1.5	0.6
14	236.8	23.4	7.1	43.6	50.4	70.4	86.4	9.1	3.9	2.7	1.3
15	221.4	33.9	NA	NA	NA	NA	NA	NA	NA	NA	NA
16	213.9	41.6	NA	NA	NA	NA	NA	NA	NA	NA	NA
17	214.6	25.7	3.6	22.4	22.6	17.1	11.1	7.8	4.9	2.4	1.5
18	216.9	51.3	NA	NA	NA	NA	NA	NA	NA	NA	NA
19	251.0	22.9	7.1	8.2	4.5	4.2	5.4	6.3	3.7	2.3	1.0
20	251.3	21.9	7.9	10.2	7.3	10.8	17.7	6.7	3.8	2.2	1.2
21	246.3	18.6	7.4	11.5	8.2	8.5	13.0	7.1	4.7	2.8	1.5
22	243.1	17.0	6.9	15.8	20.5	33.2	53.2	7.0	5.1	3.2	1.3
23	241.6	20.9	NA	NA	NA	NA	NA	NA	NA	NA	NA
24	249.1	20.6	6.6	14.4	20.8	18.5	20.7	9.4	4.1	2.7	1.9
25	248.8	21.3	6.4	10.6	13.1	21.6	29.5	8.0	3.9	2.0	1.9

NA = Not Available
a) Isp = Theoretical specific impulse
b) Measured at 1000 psi
c) All ignition times at specified laser flux (cal/cm^{2}s), measured at 250 psi.

correlations with pyrolysis product distributions.

Pyrolysis-Product/Ignition-Data Correlations: To identify correlations, several techniques and tools were used. These include simple visual examination of P-GC-FTIR data in formats similar to those used for Tables 2 and 3, as well as a multitude of plots generated by a spreadsheet program (Symphony) and two multivariate analysis packages (Ein*Sight and Minitab). Possible correlations for all pyrolysis products versus all ignition data were explored. The only correlation observed was that of total permanent gases (low temperature pyrolysis) versus go/no-go ignition time (60 cal/cm^{2}s). A plot of this data is given in Figure 1. The most general explanation for these findings is that "clean" burning samples produce small decomposition products such as CO_2, N_2O, etc., rather than large fragments such as triazine, ketones, etc. The result of this efficient decomposition process is a higher surface temperature and a shorter go/no-go ignition time.

Correlation of total permanent gases production with go/no-go ignition times at laser fluxes greater than 60 cal/cm^{2}s were also observed, but were not as good as that for the lowest laser flux, presumably due

FIGURE 1

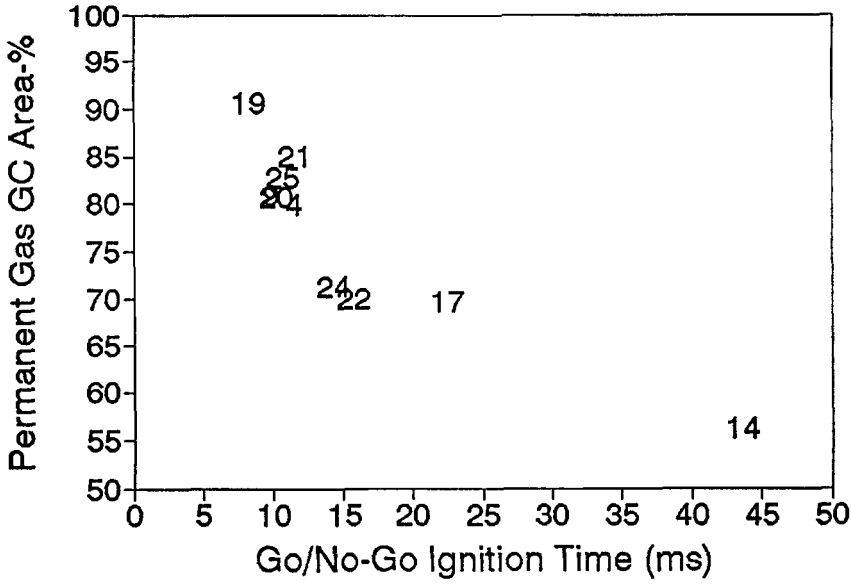

Correlation Plot. Low temperature permanent gas products vs. Go/no-go ignition time (laser flux: 60 cal/cm^{2}s).

to ablation and/or overdriven ignition[21] at the higher fluxes. No significant correlations were observed for any of the high temperature pyrolysis products when plotted against either go/no-go or first light ignition times, nor were any observed for low temperature products when plotted against first light ignition times.

DISCUSSION

There are several striking differences in the low temperature pyrolysis product distributions for RDX and HMX formulations. Most are likely due to differences in reaction temperature. All RDX based formulations were pyrolyzed at a set temperature that was 100°C lower than for HMX formulations. This was done to compensate for the difference in oxidizer melting points (204°C and 280°C for RDX and HMX, respectively). Since HMX and RDX rapidly decompose at their melting points, HMX is at a temperature 100°C higher than RDX when it actually melts. This could explain the large difference in permament gas yields between RDX and HMX, i.e. 29.9 and 92.1 area-%, respectively.

Examination of go/no-go ignition times as a function of laser flux suggests that samples can be divided into three groups. Group I, composed of samples 14, 22, 25, and 24, exhibits increasing go/no-go times with

increasing flux. Group II, composed of samples 20, 21, 4, 9, and 19, has ignition times that first decrease and then increase with increasing flux. Group III, composed only of sample 17, exhibits go/no-go ignition times that decrease with increasing laser flux. Observations described below suggest that differences in ignition behavior exhibited by these groups are related to ablation and/or overdriven ignition at high laser fluxes, as well as to the ability of plasticizer and/or plasticizer decomposition products to catalyze propellant decomposition.

Pyrolysis GC-FTIR investigation of BTTN and TMETN decomposition at 400°C reveals the production of permanent gases, including a relatively large amount of formaldehyde, as well as several nitrate ester fragments. Which, if any, of these products may serve as catalysts has not been determined, though formaldehyde has been reported to catalyze the thermal decomposition of RDX.[22-24] It is suspected that catalysis by plasticizer and/or plasticizer decomposition products in the series of LOVA propellants examined in this investigation is responsible for the production of triazine is produced by HMX formulations and unplasticized RDX formulations in low temperature experiments, as well as

by all HMX and RDX formulations in high temperature experiments, but not by plasticized RDX formulations at low temperature. In addition, nitrate esters and formaldehyde are only observed in the pyrolysis product distributions of those samples that do not generate triazine, suggesting that nitrate esters and/or formaldehyde are catalyzing the decomposition of RDX as illustrated in Scheme 1. (In a related study that used GC-MS to examine the thermal decomposition of RDX[25], it was found that the presence of borohydride catalysts eliminated both triazine oxide and NO_2 from the decomposition products.)

Inspection of the composition of samples in Groups I, II, and III reveals that Group I is composed of one unplasticized formulation and three TMETN-plasticized formulations, while Group II is composed of four BTTN-plasticized formulations and one TMETN-plasticized formulation. (The TMETN-plasticized formulation in Group II differs greatly from the other TMETN-plasticized formulations in that it contains approximately 6 wt-% more oxidizer, 10 wt-% less GAP, and 2 wt-% more TMETN.) In considering the significance of these groupings, one notes that although both BTTN and TMETN are energetic plasticizers, BTTN is the more sensitive

SCHEME 1

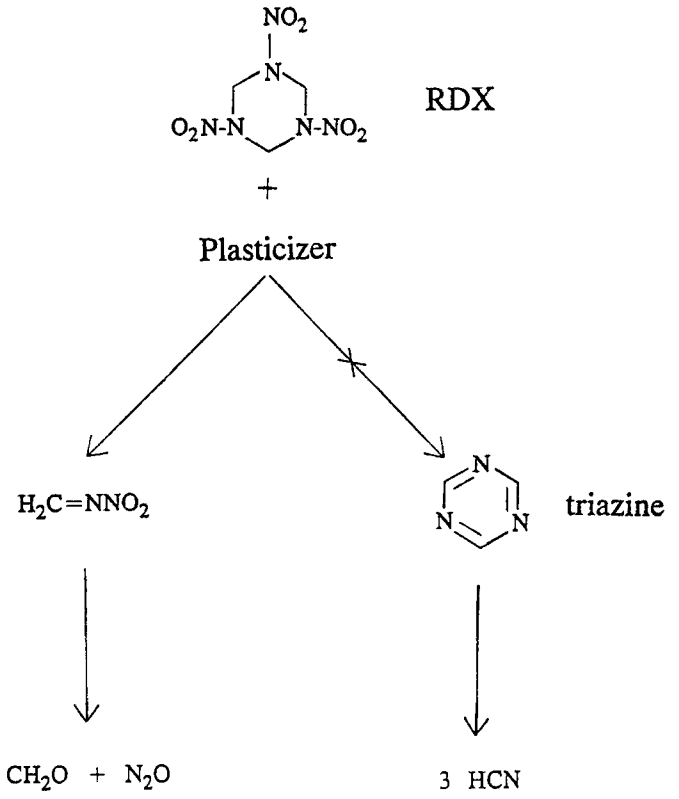

Catalysis of nitramine decomposition by nitrate ester plasticizer.

(compare impact sensitivities of samples 15 and 18 in Table 8) and is likely to decompose more readily at lower laser fluxes than will TMETN, generating decomposition products that can potentially catalyze the decompostion of the remaining sample. At high laser fluxes, ablation is a problem for all BTTN and TMETN plasticized formulations, resulting in increased ignition times. The observation that samples plasticized with BTTN tend to have shorter first light times than unplasticized formulations, or those plasticized with TMETN, may lend further support the ideas proposed here.

Plasticizers also appears to affect the decomposition of GAP in samples 15 and 18. In the low temperature experiment, sample 15 (GAP/BTTN) produces large amounts of permanent gases, but no acetaldehyde, indicating relatively complete decomposition of GAP. Sample 18 (GAP/TMETN), however, produces high levels of acetaldehyde and low levels of permanent gas, indicating less complete decomposition. In high temperature experiments, where plasticizer decomposition is probably instantaneous, catalysis of GAP decomposition is not observed, and both samples 15 and 18 generate low levels of permanent gases and almost as much acetalde-

hyde as unplasticized GAP.

Sample 17 does not fit into either Group I or II, and is the only sample that demonstrates decreasing ignition times with increasing flux. This suggests that ablation is not a problem for this unplasticized, HTPB-bound formulation. Two additional unplasticized, HTPB-bound samples[17] prepared along with those in this study, but not examined by us, show a similar trend and indicate that the behavior is not unique to sample 17, but rather is a characteristic of HTPB-bound formulations.

CONCLUSION

The primary objective of this investigation was to identify correlations between ignition times and pyrolysis product distributions. A correlation has been found for go/no-go ignition times, but not for first light ignition times. The reason for lack of correlation with first light measurements is not clear. An explanation is not necessary for a non-mechanistic study such as this, but would contribute to a more complete understanding of the systems being examined. The correlation identified was that of total permanent gases and go/no-go ignition time, and provides a means for predicting go/no-go ignition times.

Several trends in pyrolysis product distribution as a function of propellant composition have been observed. Most of these trends are believed to be related to the ability of BTTN and TMETN to catalyze decomposition. Although not directly applicable to performance prediction, the trends and observations reported here are expected to be of use to those interested in formulation design or propellant decomposition.

ACKNOWLEDGEMENT

We thank Dr. Rena Y. Yee of Naval Weapons Center, China Lake, for providing samples and performance test results used in this study.

REFERENCES

1. R.A. Fifer, in "Fundamentals of Solid Propellant Combustion, K.K. Kuo and M. Summerfield Eds., Vol. 90 of "Progress in Astronautics and Aeronautics Series, AIAA, NY, 1984.
2. M.A. Schroeder, BRL-TR-2659, June 1985.
3. M.A. Schroeder, "Proceedings of the 25th JANNAF Combustion Meeting", CPIA Pub. 498, Vol. III, pp. 421-431, 1988.

4. R.A. Fifer, S.A. Liebman, P.J. Duff, K.D. Fickie, and M.A. Schroeder, "Proceedings of the 22nd JANNAF Combustion Meeting", CPIA Pub. 432, Vol. II, pp. 537-546, Oct. 1985; see also J. Haz. Mat., Vol.13, pp. 51-56., 1986.
5. P.J. Duff, "Proceedings of the 22nd JANNAF Combustion Meeting", CPIA Pub. 432, Vol. II, pp. 547-556, Oct. 1985.
6. M.A. Schroeder, "Proceedings of the 23rd JANNAF Combustion Meeting", CPIA Pub. 457, Vol. II, pp. 43-54, Oct. 1986.
7. M.A. Schroeder, "Proceedings of the 24th JANNAF Combustion Meeting", CPIA Pub. 476, Vol. I, pp. 103-114, Oct 1987.
8. T. Tamiri and S. Zitrin, J. Energetic Materials, Vol. 4, pp 215-237.
9. J. Yinon and S. Zitrin, "The Analysis of Explosives", Pergamon Press, Oxford, 1981, Chaper 6.
10. R. Behrens, Jr., "Proceedings of the 24th JANNAF Combustion Meeting", CPIA Pub. 476, Vol. I, pp. 333-342, Oct 1987.
11. X. Zhao, E.J. Hintsa, and Y.T. Lee, J. Chem. Phys., Vol. 88, pp. 801-810, 1988.

12. A.P. Snyder, J.H. Kremer, S.A. Liebman, M.A. Schroeder, and R.A. Fifer, Organic Mass Spectrometry, Vol. 24, pp. 15-21, 1989. Organic Mass Spectrometry, Vol. 25, 61-66, 1990.

13. J.B. Morris and R.A. Fifer, "Proceedings of the 27th JANNAF Combustion Meeting", CPIA Pub. 557, Vol. I, pp. 197-211, Nov. 1990.

14. S. Wise and J.J. Rocchio, "Proceedings of the 18th JANNAF Combustion Meeting", CPIA Pub. 347, Vol. II, pp. 305-320, Oct. 1981.

15. J.K. Salo, "Proceedings of the 17th North American Thermal Analysis (NATAS) Conference", Vol. II, pp. 779-784, Oct. 1988.

16. R.Y. Yee, NWC-TP-6619, March 1985 (AD-A157 900).

17. R.Y. Yee, private communication.

18. R.Y. Yee, "Proceedings of the 1987 JANNAF Propulsion Systems Hazards Subcommittee Meeting", CPIA Pub. 464, Vol. I pp. 253-255, March 1987.

19. F.J. Shaw and R.A. Fifer, BRL-TR-2993, May 1989, "Proceedings of the 25th JANNAF Combustion Meeting", CPIA Pub. 498, Vol.III, pp. 409-420, 1988. R.A. Pesce-Rodriguez, F.J. Shaw, and R.A. Fifer, BRL-TR-3288, November 1991.

20. P.R. Griffiths and J.A. de Haseth, "Fourier Transform Infrared Spectroscopy", John Wiley & Sons: New York, pp. 604-607, 1986.
21. T.J. Ohlemiller, L.H. Caveny, L. DeLuca, and M. Summerfield, in "Proceedings of the 14th Symposium (International) on Combustion", The Combustion Institute, 20-25 August 1972.
22. D.J. Cosgrove and A.J. Owen, Combustion and Flame, Vol.22, pp.19-22, 1974.
23. J.J. Batten, Aust. J. Chem., Vol. 24, 945, 1971.
24. J.J. Batten, Aust. J. Chem., Vol. 24, 2025, 1971.
25. S.A. Liebman, A.P. Snyder, J.H. Kremer, D.J. Reutter, M.A. Schroeder, and R.A. Fifer, J. Anal.& Appl. Pyro., Vol. 12, pp. 83-95, 1987.